Available online at www.sciencedirect.com
ScienceDirect
Advances in Space Research 39 (2007) 1840–1846
ADVANCES IN SPACE RESEARCH (a COSPAR publication)
www.elsevier.com/locate/asr

What is the role of magnetic null points in large flares?

B. Schmieder [a,*], C.H. Mandrini [b], P. Démoulin [a], G. Aulanier [a], H. Li [c], A. Berlicki [d]

[a] Observatoire de Paris, LESIA, UMR 8109 (CNRS), 92195 Meudon, Cedex Principal, France
[b] Instituto de Astronomía y Física del Espacio, CONICET-UBA, CC. 67 Suc. 28, 1428 Buenos Aires, Argentina
[c] Purple Mountain Observatory, Nanjing 210008, PR China
[d] Astronomical Institute of the Wrocław University, ul.Kopernika 11, 51-622 Wrocław, Poland

Received 28 October 2006; received in revised form 15 March 2007; accepted 21 March 2007

Abstract

We have performed the analysis of the magnetic topology of active region NOAA 10486 before two large flares occurring on October 26 and 28, 2003. The 3D extrapolation of the photospheric magnetic field shows the existence of magnetic null points when using two different methods. We use TRACE 1600 Å and 195 Å brightenings as tracers of the energy release due to magnetic reconnections. We conclude on the three following points:

1. The small events observed before the flares are related to low lying null points. They are long lasting and associated with low energy release. They are not triggering the large flares.
2. On October 26, a high altitude null point is found. We look for bright patches that could correspond to the signatures of coronal reconnection at the null point in TRACE 1600 Å images. However, such bright patches are not observed before the main flare, they are only observed after it.
3. On October 28, four ribbons are observed in TRACE images before the X17 flare. We interpret them as due to a magnetic breakout reconnection in a quadrupolar configuration. There is no magnetic null point related to these four ribbons, and this reconnection rather occurs at quasi-separatrix layers (QSLs).

We conclude that the existence of a null point in the corona is neither a sufficient nor a necessary condition to give rise to large flares.

Keywords: Magnetic reconnection; Sun, magnetic fields; Sun, X-rays; Sun, flares

1. Introduction

Coronal activity such as flares, eruptions and general heating is often attributed to the manner in which the coronal field responds to photospheric motions. A very powerful tool to understand where the energy could be deposited is to study the magnetic topology of the active region, since it defines where magnetic reconnection is expected to occur (see the reviews of Démoulin, 2005; Longcope, 2005). The majority of the pioneer investigations considered a simplified two-dimensional geometry in which magnetic reconnection occurred at an isolated X-point or magnetic null point (Sweet, 1958). Field lines passing at the X-point defined two separatrices.

Baum and Bratenahl (1980) revisited this idea and proposed a 3D quadrupolar configuration, where two separatrix surfaces intercept along a single field line called the separator (which joins two magnetic null points). Magnetic reconnection does not occur only at the null points but rather along the separator in the corona. Many papers have appeared based on this 3D approach to explain flares (Démoulin et al., 1993; Mandrini et al., 1995), see Démoulin (2005) for a review. The locations of flare ribbons are understood when the separatrices are found in magnetic configurations modeled with sub-photospheric sources.

* Corresponding author.
E-mail address: Brigitte.Schmieder@obspm.fr (B. Schmieder).

0273-1177/$30
doi:10.1016/j.asr.2007.03.058

The magnetic field configuration near a null point typically shows a fan and a spine structures. Fan and spine reconnection solutions around magnetic nulls have been obtained both numerically (Craig and Fabling, 1996; Craig et al., 1999) and analytically (Ji and Song, 2001). Some flares show evidence for the existence of magnetic null points in their reconstructed magnetic configurations (Parnell et al., 1994; Aulanier et al., 2000; Manoharan and Kundu, 2005), but not all of them (Démoulin et al., 1994).

Further investigations have been done, either by increasing the number of flux tubes, modeled by magnetic sources (Longcope and Klapper, 2002), at the photospheric level or by extending the concept of separatrices to quasi-separatrices layers (QSLs) for general magnetic fields anchored to a boundary (Démoulin et al., 1996). QSLs are present where the gradients of the field line connectivity are large. QSLs generalize the definition of separatrices to cases where no coronal magnetic null is present and, so, they are the sites where magnetic field reconnection will naturally occur. This has been shown to be the case in several observed flares (Démoulin et al., 1997; Mandrini et al., 1997; Bagalá et al., 2000 and references therein). Such topological properties are insensitive to the detailed geometry of the magnetic field, and thereby create a very robust tool to understand the loci of flare energy release (see reviews of Longcope, 2005; Démoulin, 2006).

We analyze topologically an active region before very energetic flares to understand the relationship between solar flares and the existence of magnetic null points in the corona. We also test the possibility that QSLs play a similar role as null points in the reconnection process proposed by Aulanier et al. (2006). We have concentrated our study on the magnetic configuration and topology of AR 10486 before the 3B/X1.2 flare on October 26, 2003 and the X17 flare on October 28, 2003.

2. Observations

Active region NOAA 10486 (S17, L283) is one of the three main flare-productive regions that appeared in the period of October 18 through November 4, 2003 (Zhang et al., 2003). This region produced 7 X-class flares (including the largest X28 flare in GOES observational history) and 15 M-class flares during this period. This period of activity has been intensively studied. However, few papers are directly related to the magnetic configuration of this active region (Zhang et al., 2003; Régnier and Fleck, 2004; Li et al., 2006; Mandrini et al., 2006; Schmieder et al., 2006). As shown in Huairou magnetograms (Zhang et al., 2003), the AR field is highly non-potential (taking into account the direction of the transverse field), and the degree of non-potentiality is variable in different portions of the active region. This AR is characterized by strong magnetic shear, successive flux emergence, continuous sunspot rotation, and complicated magnetic topology (Li et al., 2006).

Fig. 1 shows the longitudinal magnetic field observed by THEMIS in MSDP mode in the Na D1 line at 0.24 Å from line-center starting at 08:55 UT on October 26, and at 15:23 UT on October 28 (the scan of the region took 25 min). The active region develops in a remnant one and presents mainly four polarities: the remnant negative polarity (1), the leading new polarity consisting of two sunspots (3), and two positive polarities (2 and 4) separated by a bridge of negative polarity (Fig. 1). Many satellite sunspots with different polarities appeared in the region, some of which shared their penumbra with the main sunspots, forming the δ configuration of the active region. On October 26, new bipoles emerged continuously between polarities (2) and (3); they consisted of many new magnetic elements, such as (2′) and (3′). During all this emergence new magnetic connectivities were probably established between existing and new fields. The onsets of the two flares occurred along the inversion line between the negative bridge and the positive spots (2) and (4).

3. Magnetic topology of the active region on october 26, 2003

We compute the large scale magnetic topology of the region, which is less sheared than the core field, as found in other ARs (e.g., Schmieder et al., 1996). When the magnetic shear is moderate, the separatrices and QSLs depend mostly on the distribution of the photospheric vertical field component. The effect of an increasing magnetic shear is

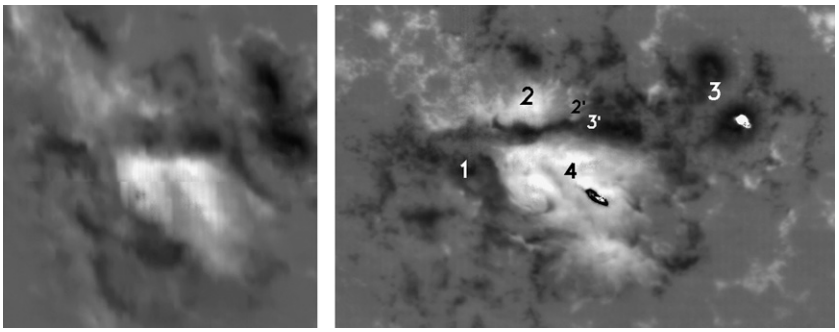

Fig. 1. THEMIS/MSDP observations showing the longitudinal magnetic field of AR NOAA 10486 on October 26, 2003 at 08:55 UT and on October 28 at 15:23 UT. The active region is formed by four main polarities (1, 2, 3, 4). The white/dark pixels in the regions of strong negative/positive field correspond to the locations of the ribbons of the X17 flare. Therefore, the magnetic field cannot be calculated correctly at these locations.

mostly to shift the spatial locations of the separatrices and QSLs. However, such an approximation is not appropriated for studying the main flare which involved a strongly sheared core field.

The photospheric magnetic field observed by THEMIS has been extrapolated using a linear force-free field model ($\vec{\nabla} \times \vec{B} = \alpha \vec{B}$) to infer the large scale 3D magnetic structure above the region. The extrapolation was performed with the code developed by Démoulin et al. (1997), which is based on a fast Fourier transform method proposed by Alissandrakis (1981). A longitudinal magnetogram of size $L \times L$ is first selected including the studied AR and its surroundings. The Fourier transform of the magnetogram introduces the spatial modes $k_x = 2\pi n_x/L$, $k_y = 2\pi n_y/L$ with n_x and n_y being positive integers (the mode $n_x = n_y = 0$, corresponding to a uniform field is supressed; this has negligible effect if the selected magnetogram has well balanced magnetic polarities and/or is large enough). The fast Fourier transform implies a periodicity in both horizontal directions (x, y), producing aliasing effects at the borders of the computational domain (see Alissandrakis (1981) for a description). The magnetic interaction of the studied domain with the periodic images is minimized taking the largest possible L and not including the magnetic connections to the lateral boundaries. Finally, the field of each mode depends with height, z, as $\exp(-lz)$ with $l = \sqrt{k_x^2 + k_y^2 - \alpha^2}$. This implies a maximum value of α ($\alpha_{\max} = 2\pi/L$) if we impose that the magnetic field should decrease to a negligible value at large heights (otherwise the large scale modes have a sinusoidal dependance with height, creating, in particular, false nulls at large heights).

The free parameter, α, of the extrapolation is usually selected by minimizing the distance between the observed loops and the computed field lines (Green et al., 2002). Alternatively, two extreme limits can be used, the potential field ($\alpha = 0$) and the maximum value ($\alpha_{\max}$). The magnetic null points are located finding numerically the roots of a system of three equations. The starting point of the finding algorithm scans a 3D mesh set on the region of interest in the extrapolated magnetic field. This procedure can be optimized by starting the search only at locations where a null point is most likely to be present (Démoulin et al., 1994).

Fig. 2(left frame) represents the extrapolation results. We use a current-free field model because we are trying to understand the origin of large scale events in the environment of AR 10486. Two magnetic null points are present in the low corona above the active region (NP2 and NP3). NP2 is in the corona (≈7 Mm) and NP3 is just above the chromosphere (≈2.3 Mm). The topology shows the typical fan and spine structures. The fan structure of NP2 is only partially depicted by the long and dark thin lines in Fig. 2. The spine field lines are shown only close to the null point; they connect to a far region, north-west of AR 10486. The fan and spine structures of NP3 are depicted by the short and dark thick lines in Fig. 2(left).

We used a second code written by M.T. Song (Song and Zhang, 2005; Song et al., 2006). It was written based on the analytical solution of Chiu and Hilton (1977), i.e., it employs the Chiu and Hilton Green functions. The boundary conditions used in our computation are the observed photospheric longitudinal field data and α. Actually, α depends on the observed photospheric field. Based on the observed photospheric vector magnetic field from Huairou Solar Observing Station, we first use the longitudinal component to compute the linear force-free field in the photosphere ($z = 0$) with different α values, and then we compare the computed transverse field with the observed one and determine the computed field that is closest to the observed one. The corresponding α value is then used as a boundary condition in our computation using MDI longitudinal field data. We use the method proposed by Zhao et al. (2005) to search for magnetic null points in the extrapolated data cube; this method employs the Poincaré index of isolated null points in a vector field. We refer the reader to Zhao et al. (2005) for a detailed description of the method.

We use $\alpha = -2.5 \times 10^{-2}\,\mathrm{Mm}^{-1}$ for the large-scale extrapolation presented in Fig. 3 (left panel). With this model we find two magnetic null points in the corona above the active region. One null point, NP1, is rather high in the corona (≈113 Mm) and another one is much lower

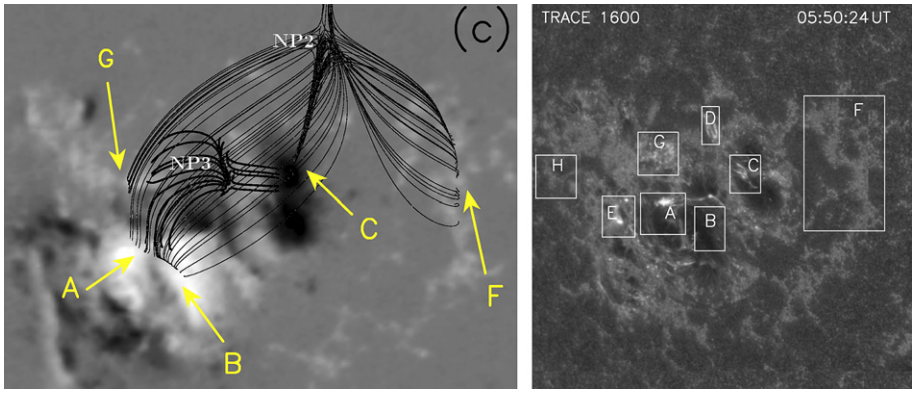

Fig. 2. Left panel: Extrapolated magnetic field lines using the longitudinal magnetic field of THEMIS on October 26 with Démoulin's code under the assumption of a current-free field. Right panel: TRACE 1600 Å image with 8 boxes marking the regions for which the light-curves are shown in Fig. 4.

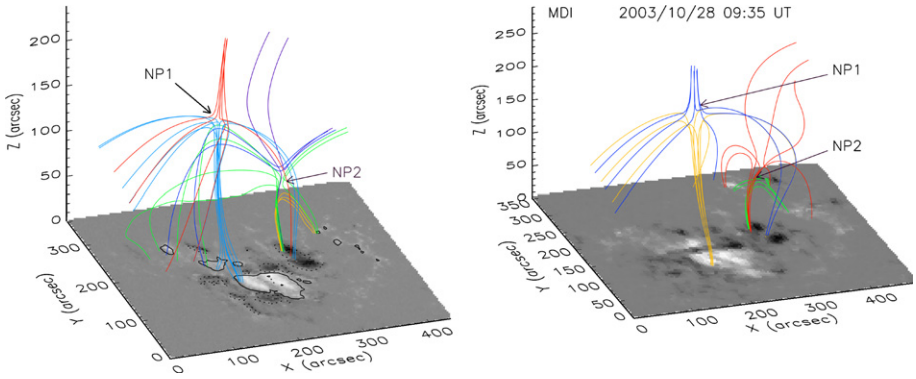

Fig. 3. Extrapolated magnetic field lines using the longitudinal magnetic field observed by MDI on October 26 (left) and 28 (right) with Song's code under the linear force-free field assumption with $\alpha = -2.5 \times 10^{-2}$ Mm^{-1} and $\alpha = -2.8 \times 10^{-2}$ Mm^{-1}, respectively.

(≈31 Mm). This later null is indeed NP2 found with the previous extrapolation. It involves the same photospheric polarities, but it is shifted to larger heights both because of a finite α value, and because a larger scale magnetogram is considered. This illustrates the influence of the extrapolation method on the location of this magnetic null and its related separatrices. Then, we can estimate the locations of regions to look for the hypothetical brightenings due to magnetic reconnection at this null point.

Both NP1 and NP2 are found at comparable locations in the extrapolation of the October 28 magnetogram (Fig. 3, right panel), so it seems that both nulls are stable and defined by the intensity and locations of the main magnetic polarities. However, NP1 was not found with the first potential extrapolation (Fig. 2, left frame). This sheds some doubt on the validity of NP1. Actually, it is an artificial null due to the linear force-free field assumption, as follows. It is well known that a linear force-free field model possess artifacts at large distances. The Chiu and Hilton Green function itself vanishes at a height $z \sim 2.8/\alpha$ due to the oscillatory nature of the linear force-free field at large distances. To check the validity of the null points detected in our extrapolated data, we take two other α values, -1.6×10^{-2} Mm^{-1} and -1.2×10^{-2} Mm^{-1}. The null point NP2 stays approximately at the same location in all three cases. However, NP1 changes its height with α and the height is very close to $2.8/\alpha$, while its location in the X and Y direction does not change. Therefore, NP1 is an artificial null point due to the linear force-free field assumption.

Does magnetic reconnection occur before the main flare at the high altitude null point as proposed by the magnetic breakout model for the initiation of CMEs (Antiochos et al., 1999)? This model invokes the presence of a magnetic null point at coronal heights above a highly sheared arcade, where reconnection could occur in a quadrupolar magnetic field configuration. The reconnection process decreases the magnetic field tension on the arcade and lets it erupt. As a consequence of reconnection, brightenings in the chromosphere could be expected at the separatrix locations. Even though the energy release at this time would be much weaker than in the main phase of the flare, weak brightenings are expected. The study of the magnetic topology gives us the location of these possible ribbons.

TRACE 1600 Å images display several bright areas before the flare onset (Fig. 2, right panel: regions A, C, D, E and G). The light-curves of these regions are presented in Fig. 4. The brightness of these regions shows a fast increase around 05:50 UT in both 1600 and 195 Å. The enhanced brightness (emission) in these regions provides evidence for magnetic reconnection at NP3, its fan and spine intersect the photosphere in regions A, C, D, and G. This reconnection should occur before the main X1.2 flare (at 06:12 UT). However, Li et al. (2006) showed that reconnection at NP3 is not physically connected to this major flare; the energy release process occurred, independently of the flare, in a limited region at low heights.

The fan of NP2 reaches the photosphere in regions A, B, F, and G and the spine in region C. However, no bright patch was observed in these regions before the flare. But, just after the flare, bright TRACE 1600 Å patches were observed, suggesting that magnetic reconnection occurred at NP2 at the flare time due to the eruption of lower magnetic field lines. Therefore, reconnection is just a byproduct of the large 3B/X1.2 flare rather than its trigger. This warns us that we should be very cautious when interpreting the observed flare precursors, since the precursor brightenings are only associated with the low-altitude null point (NP3), independent of the main flare, and not with the high-altitude null point (NP2) as the magnetic breakout model would predict.

4. Magnetic topology of the active region on October 28, 2003

On October 28, we are able to identify four ribbons already at 10:14 UT, and they are present until the large X17 flare occurrence (ribbons, R1, R2, R3, R4 in Fig. 5). The problem is to determine if a reconnection process can occur in the quadrupolar configuration described above and can heat the chromosphere at these specific locations. We computed the coronal magnetic field under the linear (constant α) force-free field assumption using both Song's and Démoulin's codes. The latter model takes into

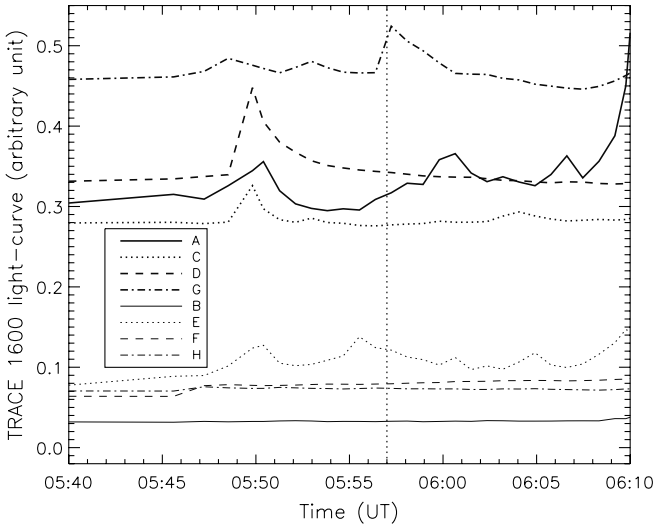

Fig. 4. TRACE 1600 Å light-curves on October 26 before the large X1.2 flare at 06:12 UT for the 8 marked regions in the right panel of Fig. 2.

account the transformation of coordinates from the AR location to disk center. The magnetic field model depends on the free parameter α. We have taken as boundary condition for our coronal model the MDI magnetogram closest in time to the X17 flare.

Our first attempt was to use Song's code taking $\alpha = -2.8 \times 10^{-2}\,\mathrm{Mm}^{-1}$. We found no magnetic null point to explain the locations of the four ribbons since NP2 is associated with the topology of the field at large scales (partly rooted outside AR 10486, Fig. 3, right panel). Next, since the magnetic field is highly non potential, we show the results with the highest possible value of α, α_{max}, allowed by Démoulin's code for a size of our integration box that includes all the AR polarities, and is large enough to avoid aliasing effects (Démoulin et al., 1997; Green et al., 2002). This value is $\alpha = -1.6 \times 10^{-2}\,\mathrm{Mm}^{-1}$. We found a good fit between the computed magnetic field lines (Fig. 5, right panel) and the loops observed by TRACE in 195 Å, described in Mandrini et al. (2006). But, also in this approach, we could not find a magnetic null point to explain the observed four ribbons (another null point is also found on the October 28, but it gives a magnetic topology which is too localized; see the end of this section).

Still, the magnetic field model gave us information about the magnetic complexity of the AR in the corona and allowed us to find clues about the location of possible reconnection sites, as discussed below. The field lines in Fig. 5 (right panel) have been computed starting integration at the photosphere within the four polarities described above (1, 2, 3, 4). It can be seen that the computed field lines connect the kernels in pairs. The continuous thin field lines to the east connect the elongated kernel lying along polarity 2 to the U shape kernel on polarity 1, while the ones to the south-west connect the compact kernel at the south of polarity 3 to the extended kernel lying to the east of polarity 4. In an analogous way, kernels lying on 2 and 3 can be connected by the thick field lines to the north, while those lying on 1 and 4 are linked by the thick field lines to the south. We have obtained similar results using the linear

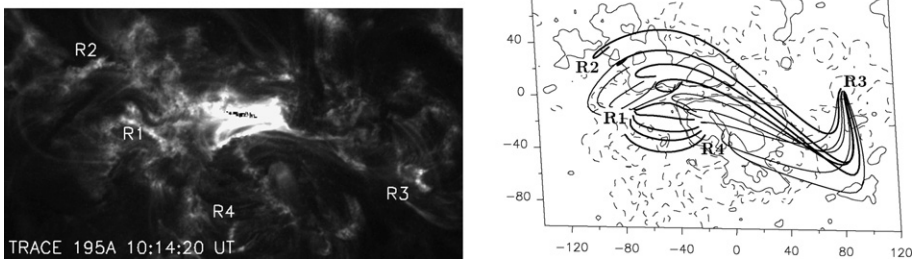

Fig. 5. TRACE image in 195 Å and extrapolated magnetic field lines over the MDI magnetogram of AR 10486 on October 28, 2003 (grey thin/black thick lines before/after the reconnection). The figure shows the four ribbons for the large-scale event: (R1, R3, R4, R6). The axes are labeled in Mm and the isocontours of the field correspond to ±100, 1000 G in thin continuous (dashed) lines for the positive (negative) values.

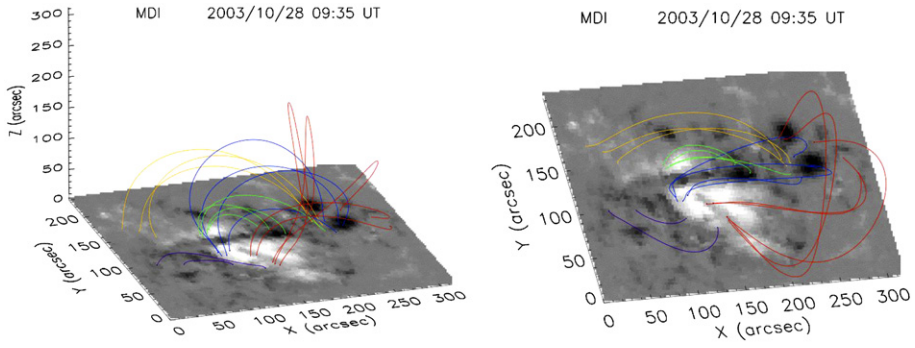

Fig. 6. Extrapolated field lines over the active region on October 28, 2003, using the Song's code. Left panel, perspective view; right panel, projected view.

force-free field extrapolation given by Song's code (Fig. 6). This coronal connectivity combined with the evolution observed in UV with TRACE strongly suggests that the four kernels are the result of magnetic field reconnection occurring at coronal heights.

The brightening of the four main ribbons can be explained in the context of the magnetic breakout model (Antiochos et al., 1999). However, we have not found such a null point in connection to the field lines that link the four observed kernels. Instead, we have found the ribbons at the end of the four magnetic connectivities shown in Fig. 5. QSLs are defined as thin volumes in which field lines display locally strong connectivity gradients, as shown in Fig. 5. Recent papers have shown that strong electric current layers are present at QSLs (Aulanier et al., 2005, 2006; Büchner, 2006; de Moortel and Galsgaard, 2006). Following these studies we propose that, in this particular example, reconnection occurs at QSLs (instead of at a magnetic null point), being the evolution predicted by the magnetic breakout model still fully consistent with our observations.

Finally, the brightest region observed in the middle of the left panel of Fig. 5 corresponds to a small flare. We have found a low null point similar to the low altitude NP3 on October 26, 2006 (Fig. 2, left panel). Magnetic reconnection occurring at this null point permits us interpret the small flare ribbons and loops observed with TRACE 1600 Å and 195 Å filters. This small flare has no relationship to the large X17 flare (Mandrini et al., 2006), contrary to the four ribbons identified above.

5. Conclusion

We analyze the potential role of magnetic null points in large flares studying a powerful active region, AR 10486, on October 26 and 28, 2003. The aim of this work is to check if such null points have the importance that some theories give them in the flare process. More precisely, we check if a null point is present in the magnetic configuration where large flares occur. If the answer is positive, we check if its associated magnetic topology can explain the spatial organization of the observed flare brightenings (ribbons, loops).

The determination of magnetic null points relies on the coronal extrapolation of the observed photospheric field. The presence of nulls can, a priori, depend on the type of technique used. Then, we compare the results of two numerical codes. Both use a linear force free field, but differ in the method (Green functions and fast Fourier transform). The two methods have different biases, in particular for the determination of null points. Both codes have been successfully used before to interpret various observations. In particular, linear force-free extrapolations were shown to be sufficient to understand the spatial organization of ribbons in many flares where separatrices and/or QSLs were computed from the extrapolations.

From the two different extrapolation methods we find three null points, NP1, NP2 and NP3, in the magnetic configuration of AR 10486. NP1 is at the largest height and it is an artificial null due to the linear force-free field assumption (linked to the spatial oscillations of such field at large distances). NP2 is relatively high, but no flaring emission is associated to this null point. NP3 is low (few Mm above the photosphere) and it is well associated to confined small flares (brightenings and heated loops are observed in the vicinity of its fan/spine) (Luoni et al., in press).

However, we show that the existence of magnetic null points has no crucial role in triggering the main flares on October 26 and 28, 2003 (an X1.2 flare and X17 flare, respectively). The location of the brightenings and loops of the pre-events are explained by the magnetic topology of a low lying magnetic null point (NP3 on October 26). However, the pre-events of the X1.2 flare on October 26 were not precursors of this large flare. Two days later, a magnetic null point was still present at low altitudes. Reconnection at this null point can only explain the observed small flare. The large flare was produced independently of the presence of the null point (Mandrini et al., 2006).

One pre-event of the flare on October 28 was recognized to be a precursor of the main flare, opening the overlaying field lines by a magnetic breakout mechanism before the main energy release. However, the reconnection occurred at quasi-separatrix layers (QSLs) rather than at a null point or at separatrices.

Therefore, we conclude that the presence of magnetic null points does not always lead to the occurrence of flares, in agreement with the conclusions of Aulanier et al. (2006) derived from 3D MHD simulations. Moreover, low energy release occurring nearby and before the main flare, usually called a pre-event, is not always triggering the main flare.

Acknowledgements

SOHO is a joint project of ESA and NASA, and THEMIS is a French-Italian telescope operated on the island of Tenerife by the CNRS-CNR in the Spanish Observatorio del Teide of the Instituto de Astrofísica de Canarias. We are grateful to the THEMIS team which operates the telescope at Tenerife. The magnetic field extrapolations used in this paper were obtained from the code base FRench Online MAGnetic Extrapolations (FROMAGE). FROMAGE is a joint project between LESIA (Observatoire de Paris), CPhT (Ecole Polytechnique), and the Centre National d'Etudes Spatiales (CNES). The work of H.L. was supported by the National Natural Science Foundation of China (NSFC, Grant Nos. 10333040 and 10573038) and National Basic Research Priorities Project (2006CB806302) of China, and that of A.B. and B.S. by the European Commission through the RTN programme (European Solar Magnetism Network, contract HPRN-CT-2002-00313). This work was partially supported by the French–Chinese contract (CNRS-CAS No. 16304).

B.S., C.H.M. and P.D. acknowledge financial support from CNRS (France) and CONICET (Argentina) through their cooperative science program (05ARG0011 N^0 18302). C.H.M. thanks the Argentinean Grants: UBACyT X329 (UBA), PICT 12187 (ANPCyT) and PIP 6220 (CONICET). C.H.M is a member of the Carrera del Investigator Científico (CONICET). The work of A.B. was supported by the Polish Ministry of Science and Higher Education, Grant No. N203 016 32/2287.

References

Alissandrakis, C.E. On the computation of constant alpha force-free magnetic field. A&A 100, 197–200, 1981.

Antiochos, S.K., DeVore, C.R., Klimchuk, J.A. A model for solar coronal mass ejections. ApJ 510, 485–493, 1999.

Aulanier, G., DeLuca, E.E., Antiochos, S.K., McMullen, R.A., Golub, L. The topology and evolution of the Bastille Day Flare. ApJ 540, 1126–1142, 2000.

Aulanier, G., Pariat, E., Démoulin, P., Devore, C.R. Slip-running reconnection in quasi-separatrix layers. Solar Phys. 238, 347–376, 2006.

Aulanier, G., Pariat, E., Démoulin, P. Current sheet formation in quasi-separatrix layers and hyperbolic flux tubes. A&A 444, 961–976, 2005.

Bagalá, L.G., Mandrini, C.H., Rovira, M.G., Démoulin, P. Magnetic reconnection; a common origin for flares and AR interconnecting arcs. A&A 363, 779–788, 2000.

Baum, P.J., Bratenahl, A. Flux linkages of bipolar sunspot groups – a computer study. Solar Phys. 67, 245–258, 1980.

Büchner, J. Locating current sheets in the Solar Corona. Space Sci. Rev. 122, 149–160, 2006.

Chiu, Y.T., Hilton, H.H. Exact Green's function method of solar force free magnetic-field computations with constant alpha. I – Theory and basic test cases. ApJ 212, 873–885, 1977.

Craig, I.J.D., Fabling, R.B., Heerikhuisen, J., Watson, P.G. Magnetic reconnection solutions in the presence of multiple nulls. ApJ 523, 838–848, 1999.

Craig, I.J.D., Fabling, R.B. Exact solutions for steady state, spine, and fan magnetic reconnection. ApJ 462, 969–976, 1996.

Démoulin, P., Bagaléa, L.G., Mandrini, C.H., Hénoux, J.C., Rovira, M.G. Quasi-separatrix layers in solar flares. II. Observed magnetic configurations. A&A 325, 305–317, 1997.

Démoulin, P., Hénoux, J.C., Mandrini, C.H. Are magnetic null points important in solar flares? A&A 285, 1023–1037, 1994.

Démoulin, P., Hénoux, J.C., Priest, E.R., Mandrini, C.H. Quasi-separatrix layers in solar flares. I. Method. A&A 308, 643–655, 1996.

Démoulin, P., van Driel-Gesztelyi, L., Schmieder, B., Hénoux, J.C., Csepura, G., Hagyard, M.J. Evidence for magnetic reconnection in solar flares. A&A 271, 292–307, 1993.

Démoulin, P. Magnetic topologies: where will reconnection occur? in: Innes, D.E., Lagg, A., Solanki, S.A. (Eds.), ESA SP-596: Chromospheric and Coronal Magnetic Fields, 2005.

Démoulin, P. Extending the concept of separatrices to QSLs for magnetic reconnection. Adv. Space Res. 37, 1269–1282, 2006.

de Moortel, I., Galsgaard, K. Numerical modelling of 3D reconnection due to rotational footpoint motions. A&A 451, 1101–1115, 2006.

Green, L.M., López fuentes, M.C., Mandrini, C.H., Démoulin, P., Van Driel-Gesztelyi, L., Culhane, J.L. The magnetic helicity budget of a cme-prolific active region. Solar Phys. 208, 43–68, 2002.

Ji, H.S., Song, M.T. Three-dimensional solutions for fan and spine magnetic reconnection in partially ionized plasmas. ApJ 556, 1017–1026, 2001.

Li, H., Schmieder, B., Aulanier, G., Berlicki, A. Is pre-eruptive null point reconnection required for triggering eruptions? Solar Phys. 237, 85–100, 2006.

Longcope, D.W., Klapper, I. A general theory of connectivity and current sheets in coronal magnetic fields anchored to discrete sources. ApJ 579, 468–481, 2002.

Longcope, D.W. Topological methods for the analysis of solar magnetic fields. Living Rev. Solar Phys. 2, 1–58, 2005.

Luoni, M., Mandrini, C.H., Cristiani, G., Démoulin, P. The magnetic field topology associated with two M flares. Adv. Space Res., in press. doi:10.1016/j.asr.2007.02.005.

Mandrini, C.H., Démoulin, P., Bagalá, L.G., van Driel-Gesztelyi, L., Hénoux, J.C., Schmieder, B., Rovira, M.G. Evidence of magnetic reconnection from Hα, soft X-ray and photospheric magnetic field observations. Solar Phys. 174, 229–240, 1997.

Mandrini, C.H., Démoulin, P., Rovira, M.G., de La Beaujardiere, J.-F., Hénoux, J.C. Constraints on flare models set by the active region magnetic topology of AR 6233. A&A 303, 927–939, 1995.

Mandrini, C.H., Démoulin, P., Schmieder, B., Deluca, E.E., Pariat, E., Uddin, W. Companion event and precursor of the X17 Flare on 28 October 2003. Solar Phys. 238, 293–312, 2006.

Manoharan, P.K., Kundu, M.R. Multi-wavelength study of a coronal mass ejection: a flare event from AR 9393. Adv. Space Res. 35, 70–74, 2005.

Parnell, C.E., Priest, E.R., Golub, L. The three-dimensional structures of X-ray bright points. Solar Phys. 151, 57–74, 1994.

Régnier, S., Fleck, B. The magnetic field evolution of AR 10486 and AR 10488 before and after the X17 Flare on Oct. 28, 2003, in: Bulletin of the American Astronomical Society, pp. 668–672, 2004.

Schmieder, B., Démoulin, P., Aulanier, G., Golub, L. Differential magnetic field shear in an active region. ApJ 467, 881–886, 1996.

Schmieder, B., Mandrini, C.H., Démoulin, P., Pariat, E., Berlicki, A., DeLuca, E. Magnetic reconfiguration before the X 17 Solar flare of October 28 2003. Adv. Space Res. 37, 1313–1316, 2006.

Song, M.T., Fang, C., Tang, Y.H., Wu, S.T., Zhang, Y.A. A new and fast way to reconstruct a nonlinear force-free field in the Solar Corona. ApJ 649, 1084–1092, 2006.

Song, M.T., Zhang, Y.A. Comments on solar linear force-free field and application of FFT analysis. ChA&A 29, 159–180, 2005.

Sweet, P.A. The neutral point theory of Solar Flares, in: IAU Symp. 6: Electromagnetic Phenomena in Cosmical Physics, p. 123, 1958.

Zhang, H.-Q., Bao, X.-M., Zhang, Y., Liu, J.-H., Bao, S.-D., et al. Three super active regions in the descending phase of Solar cycle 23. Chinese J. Astron. Astrophys. 3, 491–494, 2003.

Zhao, H., Wang, J.-X., Zhang, J., Xiao, C.-J. A new method of identifying 3D null points in Solar vector magnetic fields. Chinese J. Astron. Astrophys. 5, 443–447, 2005.